ACS APPLIED MATERIALS & INTERFACES

Letter

www.acsami.org

Emulsion Synthesis of Size-Tunable $CH_3NH_3PbBr_3$ Quantum Dots: An Alternative Route toward Efficient Light-Emitting Diodes

Hailong Huang,[†,‡,#] Fangchao Zhao,[§,#] Lige Liu,[†] Feng Zhang,[†] Xian-gang Wu,[†] Lijie Shi,[‡] Bingsuo Zou,[‡] Qibing Pei,[*,§] and Haizheng Zhong[*,†]

[†]Beijing Key Laboratory of Nanophotonics and Ultrafine Optoelectronic Systems, School of Materials Science & Engineering, [‡]Micro Nano Technology Center, School of Physics, Beijing Institute of Technology, 5 Zhongguancun South Street, Haidian District, Beijing 100081, China

[§]Department of Materials Sciences and Engineering, California NanoSystems Institute, Henry Samuli School of Engineering and Applied Science, University of California, Los Angeles, California, United States

Supporting Information

ABSTRACT: We report a facile nonaqueous emulsion synthesis of colloidal halide perovskite quantum dots by controlled addition of a demulsifier into an emulsion of precursors. The size of resulting $CH_3NH_3PbBr_3$ quantum dots can be tuned from 2 to 8 nm by varying the amount of demulsifier. Moreover, this emulsion synthesis also allows the purification of these quantum dots by precipitation from the colloidal solution and obtains solid-state powder which can be redissolved for thin film coating and device fabrication. The photoluminescence quantum yields of the quantum dots is generally in the range of 80−92%, and can be well-preserved after purification (∼80%). Green light-emitting diodes fabricated comprising a spin-cast layer of the colloidal $CH_3NH_3PbBr_3$ quantum dots exhibited maximum current efficiency of 4.5 cd/A, power efficiency of 3.5 lm/W, and external quantum efficiency of 1.1%. This provides an alternative route toward high efficient solution-processed perovskite-based light-emitting diodes. In addition, the emulsion synthesis is versatile and can be extended for the fabrication of inorganic halide perovskite colloidal $CsPbBr_3$ nanocrystals.

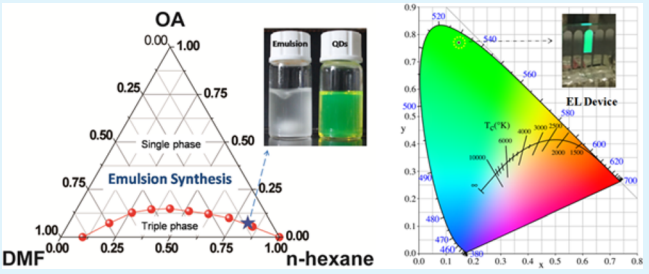

KEYWORDS: *emulsion synthesis, quantum dot, semiconductor nanocrystals, halide perovskite, light-emitting diodes, electroluminescence*

Organometal halide perovskites ($CH_3NH_3PbX_3$, X = Cl, Br, I) are inexpensive materials with desirable optical and electrical characteristics suitable for solar-harvesting and light-emitting applications.[1] Beyond well-developed perovskites based solar cells, the high photoluminescence quantum yields (PLQYs) and broad color-tunability of halide perovskites also evoke the exploration of their use as emissive materials in light-emitting diodes (LEDs),[2−5] lasers,[6−8] and optical sensors.[9] It has been suggested that nanosized halide perovskites exhibit enhanced PL properties and device performance.[10−12] Although previous works have been mostly focused on nanostructured thin films,[12−15] the study of nanosized halide perovskites in colloidal solution is limited.

Very recently, colloidal perovskite quantum dots (QDs) with enhanced PL properties had been successfully fabricated through simple reprecipitation method or by adapting the hot injection methods.[16−21] On the basis of the successes of QD-LEDs, these $CH_3NH_3PbX_3$ perovskite QDs stabilized with long-chain surfactants are attractive new emissive materials and provide an alternative route for fabricating electroluminescence (EL) devices using spin-casting or printing techniques.[22−24] However, colloidal QDs must be carefully purified to remove excess precursors and surfactants before the integration into devices, as these residues are detrimental to the PL efficiency and device performance. Unfortunately, $CH_3NH_3PbX_3$ perovskites are unstable in many polar solvents such as N, N-dimethylformamide (DMF), methanol, and ethanol. The purification of these QDs from colloidal solution using common reprecipitation technique encountered a challenge of finding a suitable pair of polar and nonpolar solvents: the polar solvents would induce PL quenching or even destroy the QDs. So far, the reported techniques are not readily adaptable to purify the QDs. The lack of properly purified $CH_3NH_3PbX_3$ QDs, especially high-quality solid-state QD powder, has hindered their use in high-performance EL devices.[18]

In this work, we use two immiscible solvent (DMF and *n*-hexane) to introduce an emulsion system, which separate the two liquid into microscopic scale. The addition of demulsifier subsequently initializes solvent mixing and induces the crystallization process. This method provides better control of the crystallization process and result in monodisperse $CH_3NH_3PbBr_3$ QDs with tunable size from 2 to 8 nm and absolute PL quantum yields (PLQYs) of 80−92%. The

Received: October 28, 2015
Accepted: December 12, 2015
Published: December 12, 2015

DOI: 10.1021/acsami.5b10373
ACS Appl. Mater. Interfaces 2015, 7, 28128−28133

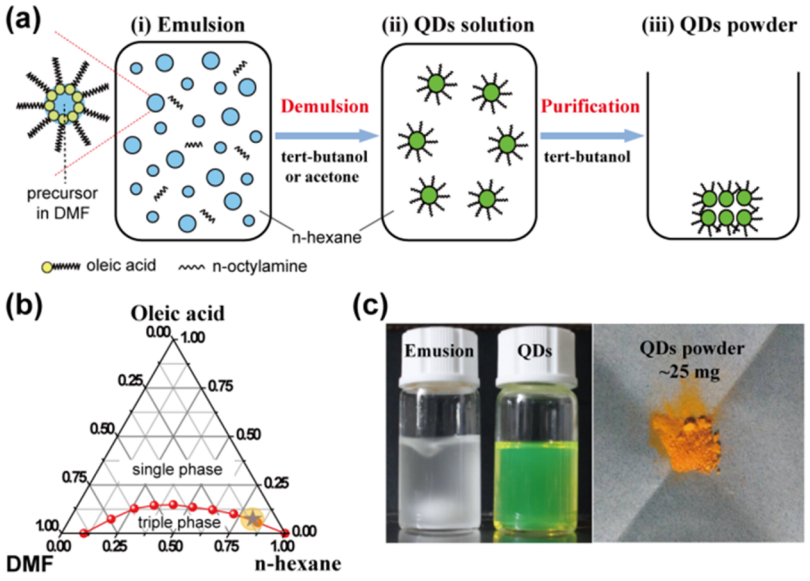

Figure 1. (a) Schematical illustration of the QD emulsion synthesis, (i) formation of the emulsion, (ii) demulsion by adding demulsifier, and redisperse into colloidal solution, (iii) purification into solid-state powder. (b) Ternary phase diagram (DMF/OA/*n*-hexane). The blue asterisk point and its coordinate indicate the mass ratio used in this work. (c) Optical photographs of typical $CH_3NH_3PbBr_3$ emulsion, resultant colloidal solution, and solid-state powder of $CH_3NH_3PbBr_3$ QDs.

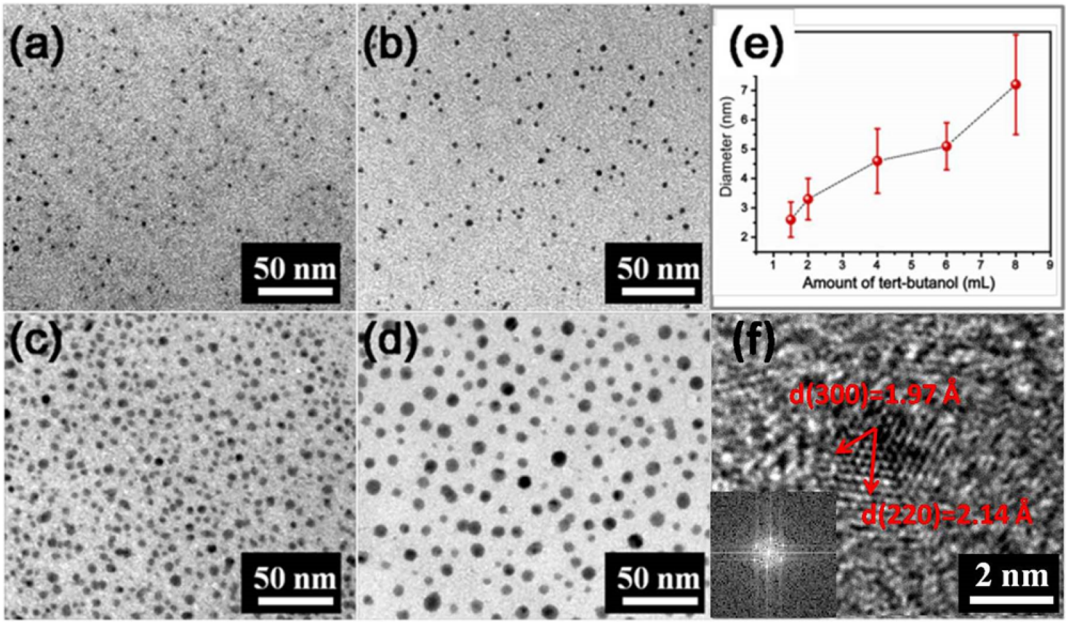

Figure 2. (a–d) Low-resolution TEM image of $CH_3NH_3PbBr_3$ QDs with diameter of 2.6 ± 0.6, 3.3 ± 0.7, 4.6 ± 1.1, and 7.2 ± 1.7 nm. (e) Plot of average diameter of resultant QDs with the amount of *tert*-butanol. (f) High-resolution TEM image of a single QD with lattice planes in two directions. Inset: FFT pattern transformed from the HRTEM image.

resultant QDs can be precipitated and isolated through a controlled demulsion process, and then purified into QD powder for further use. The purified QDs have allowed the fabrication of efficient EL devices having a simple sandwich structure. Furthermore, we extend this method for the fabrication of colloidal $CsPbBr_3$ nanocrystals.

The nonaqueous emulsion synthesis was carried out in two steps, as schematically shown in Figure 1a: emulsion formation and demulsion.[25] First, a pair of immiscible polar and nonpolar solvents as well as a surfactant were mixed to form emulsion. A demulsifier was then added to initialize the mixing of precursors. The reagents encapsulated inside the inverted micelles would become mixed with the polar solvent. The solubility change induces the formation of colloidal nanoparticles. In our system, DMF was used as the "aqueous phase", *n*-hexane as "oil phase", oleic acid (OA) as "surfactant", and *tert*-butanol as demulsifier. By adjusting the weight ratio of these three components, the mixture can be tuned from three phases to a single phase. Figure 1b shows the ternary phase diagram (DMF/OA/*n*-hexane) and the details of the plotting are described in the Supporting Information. The synthesis was accomplished in a water-in-oil emulsion system that was shown as blue asterisk point and highlighted with yellow color. To obtain $CH_3NH_3PbBr_3$ QDs, we successively dropped the

DOI: 10.1021/acsami.5b10373
ACS Appl. Mater. Interfaces 2015, 7, 28128–28133

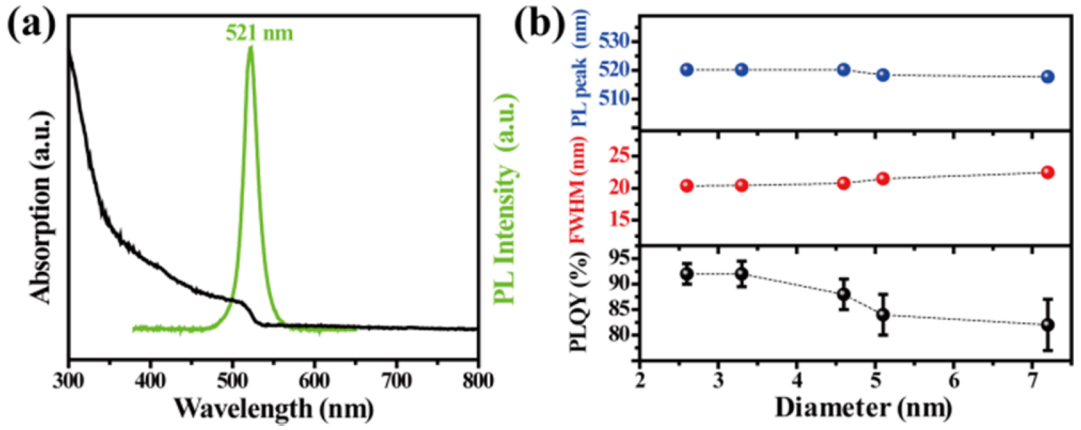

Figure 3. (a) UV−vis absorption & PL emission spectra of a typical $CH_3NH_3PbBr_3$ QD solution. (b) PL emission peak, fwhm, and PLQYs as a function of the size of $CH_3NH_3PbBr_3$ QDs.

reagents of CH_3NH_3Br (0.16 mmol CH_3NH_3Br dissolved in 0.3 mL DMF) and $PbBr_2$ (0.2 mmol $PbBr_2$ dissolved in 0.5 mL DMF) into a mixture of hexane (10 mL), OA (0.5 mL) and octylamine (20 μL). The formation of emulsion was not affected by these precursors. A certain amount of *tert*-butanol (1.5−8 mL) or acetone (8 mL) was used as demulsifier and dropped into the reaction system to initiate a demulsion process. The resulting suspension was precipitated from the solution by centrifugation at 6000 rpm for 5 min. The precipitates can be partially redissolved into a nonpolar solvent (toluene, hexane) to form colloidal solutions (see left of Figure 1c). After that, the QDs can be reprecipitated from the colloidal solution by adding a fixed amount of *tert*-butanol, and then dried into solid-state powder (see right of Figure 1c). The experimental detail is shown in the Supporting Information. Tert-butanol has two roles: demulsifier and precipitant. Because of good intermiscibility with oleic acid and octylamine, tert-butanol can decrease the surface tension of micelle between DMF and *n*-hexane that led to this two immiscible solvent mixing completely. Tert-butanol also acts a poor solvent to precipitate the QDs and remove the additional surfactants such as oleic acid and octylamine.

In the reprecipitation method, solubility change induced by solvent mixing is an essential process to drive the nucleation and crystal growth.[26] As the emulsion system provides microreactors for solvent mixing, the emulsion synthesis is advantageous to realize the size and shape control. In this work, the size control of $CH_3NH_3PbBr_3$ QDs was achieved by varying the amount of demulsifier. Figure 2a−d show the transmission electron microscopy (TEM) images of typical $CH_3NH_3PbBr_3$ QDs with average diameter of 2.6 ± 0.6 nm, 3.3 ± 0.7 nm, 4.6 ± 1.1 nm, and 7.2 ± 1.7 nm (the size analysis is shown in Figure S1). Figure S2 also shows the TEM image of the sample having average diameter of 5.1 ± 0.8 nm. As illustrated in Figure 2e, the average diameter of the $CH_3NH_3PbBr_3$ QDs and their corresponding size distribution increase with increasing amount of *tert*-butanol during the demulsion process. In contrast, the use of acetone as demulsifier only gives colloidal QDs with polydispersed nanoparticles (Figure S3). Figure 2f shows the high-resolution TEM (HRTEM) image of a single QD with good crystallinity. Closer examination illustrates two obvious intersection planes with space distances of 1.97 and 2.14 Å, which can be attributed to the (3, 0, 0) and (2, 2, 0) places of cubic $CH_3NH_3PbBr_3$. As shown in the inset of Figure 2f, fast Fourier transformation (FFT) pattern has clear spots corresponding with the lattice spacing. In addition, the two well-defined crystal faces can be clearly identified from X-ray diffraction (XRD) patterns (Figure S4).

Figure 3 shows the UV−vis absorption and PL spectra of $CH_3NH_3PbBr_3$ QDs in hexane. The UV−vis absorption spectra have an obvious excitonic absorption peak with a band edge at about 512 nm (2.42 eV). A sharp PL emission was detected at a peak of 521 nm (2.38 eV) with a narrow full width at the half-maximum (fwhm) of 21 nm. The observed small Stokes shift (~40 meV) is an obvious excitonic feature, implying that the PL emission of $CH_3NH_3PbBr_3$ QDs mainly originates from the exciton recombination.[27] The size dependence of absorption and PL properties are displayed in Figure 3b and Figure S5, no obvious change can be resolved from the absorption and PL spectra of the samples with average diameter ranging from 2.6 to 7.2 nm. According to the experimental and calculation results of size-dependent PL emission for $CH_3NH_3PbBr_3$ nanoplatelets,[28] this phenomenon of size-independency can be attributed to the weak quantum confinement effects for the sample with average size larger than 2.0 nm. We further determined the absolute PLQYs of these samples by equipping a fluorescence spectrometer with an integrated sphere to collect emission in all angles as excited at a wavelength of 450 nm. The measured PLQYs were generally in the range of 80−92% for all colloidal solutions from different batches, which are higher than samples prepared through ligand-assited reprecipitation (LARP) technique by simple solvent mixing.[18] The purification process only induce a slight decrease of the PLQYs (Figure S6), which suggest that the purified samples are still well-capped by the ligands. The high PLQY (~80%), saturated emission color (fwhm: 21 nm), and acceptable yield (~25 mg per batch) of the purified $CH_3NH_3PbBr_3$ QDs with average size of 4.6 ± 1.1 nm make it a promising candidate for light-emitting diode demonstration.

The emulsion synthesis reported here is versatile for the fabrication of other halide perovskites. We here extended this method to fabricate inorganic $CsPbBr_3$ nanocrystals. As shown in Figure S7a, the resulting $CsPbBr_3$ nanocrystals are nanocubes with size of 9−20 nm. HRTEM and XRD characterizations (Figure S7b, c) showed that these $CsPbBr_3$ nanocrystals are highly crystalline with cubic phase. UV−vis and PL determinations (see Figure S7d) demonstrated that the resulting $CsPbBr_3$ nanocubes exhibit obvious excitonic features with sharp absorption edge at about 504 nm (2.46 eV) and narrow band PL emission at 510 nm (fwhm: ~18 nm, PL peak:

DOI: 10.1021/acsami.5b10373
ACS Appl. Mater. Interfaces 2015, 7, 28128−28133

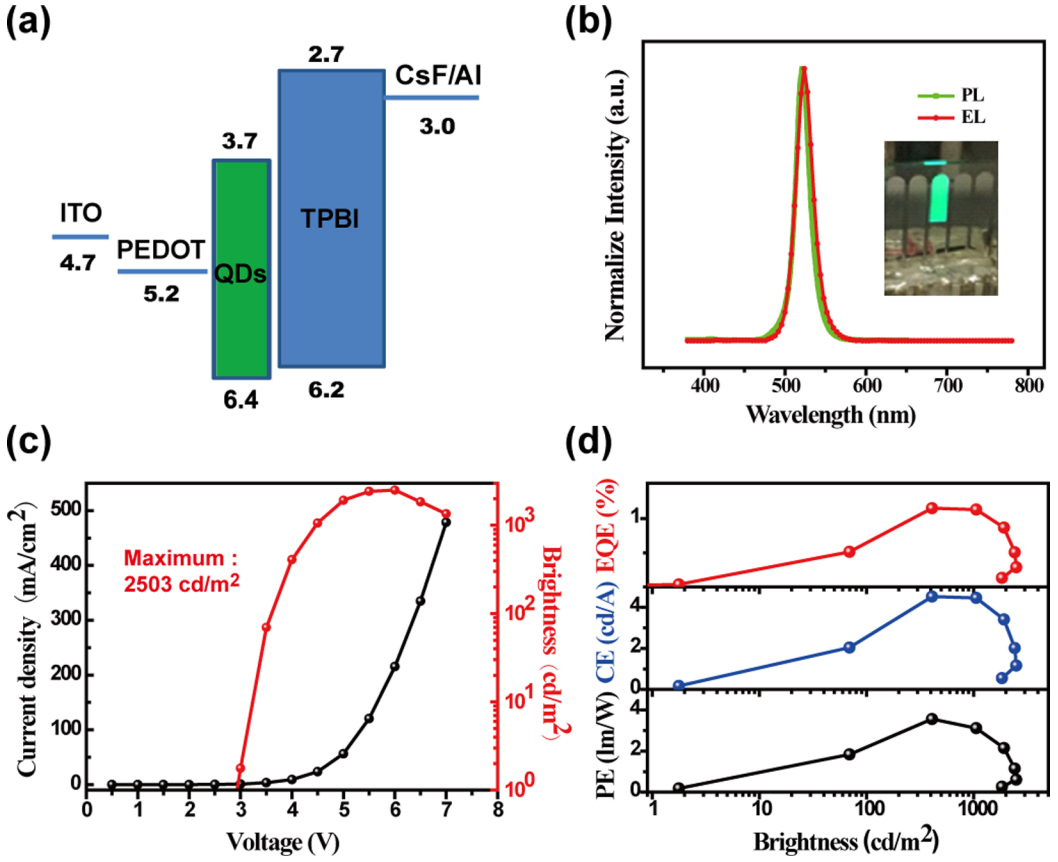

Figure 4. Characteristics of QD-LEDs. (a) Flat-band energy-level diagram of different layers of materials employed in the QD-LED. The values of energy levels are illustrated with respect to vacuum level. (b) Comparison of normalized EL (solid red line) and PL (dashed blue line) spectra of $CH_3NH_3PbBr_3$ QDs. The inset is an optical photograph of a lit QD-LED. (c) Current density (red) and brightness (blue) versus voltage characteristics. (d) Current, power efficiency, and EQE as a function of brightness of the QD-LED.

2.43 eV). The PLQYs is determined to ~60% for the optimized samples. More work is ongoing to achieve the size- and shape-tunable materials.

EL devices were fabricated with a simple thin film sandwich structure of glass/indium−tin oxide (ITO)/PEDOT:PSS(40 nm)/ $CH_3NH_3PbBr_3$ QDs/TPBi (40 nm)/CsF(1 nm)/Al(80 nm), as shown in Figure 4a. Poly(3,4-ethylenedioxythiophene):poly(styrenesulfonate) (PEDOT:PSS) was used to enhance hole injection. 1, 3, 5-tris (2-*N*-phenylbenzimidazolyl) benzene (TPBi) takes the role of electron transport layer, whereas CsF serves as the cathode buffer layer. $CH_3NH_3PbBr_3$ QDs dissolved in toluene (2.5 mg/mL) were spin-casted on to the PEDOT: PSS as green light-emitter. The surface and cross-sectional morphologies of a typical device were characterized by applying atomic force microscope (AFM) and scanning electron microscopy (SEM) characterizations (see Figure S8), illustrating the formation of uniform QDs film through spin-casting technique. The EL device shows a strong EL emission peaked at 524 nm, as shown in Figure 4b, which is slightly red-shifted compared to its PL spectrum which peaks at 521 nm. The device showed an ideal color-saturated green emission with Commission Internationale de l'Eclairage (CIE) color coordinates of (0.14, 0.77) and a narrow full width at half-maximum (fwhm) of 24 nm. Figure 4b inset displays a lit QD EL device at 120 cd/m^2 brightness. The current density-brightness-voltage characteristics of the QD-LEDs are presented in Figure 4c. The device exhibits a low turn-on voltage of 2.9 V at 1 cd/m^2, which is comparable to typical thin film QD-LEDs, but it is ~0.5 V higher than the thin film-based LEDs with optimized interfaces.[4,12] This increased turn-on voltage can be explained by the larger bandgap and thus higher injection barriers for the QDs. The brightness reaches a maximum of 2503 cd/m^2 with a current density of 120 mA/cm^2 at 5.5 V. As shown in Figure 4d, the EL device has a maximum current efficiency of 4.5 cd/A, power efficiency of 3.5 lm/W, and EQE of 1.1% at the brightness of 410 cd/m^2. It is noted that the device exhibit a lifetime of tens of minutes under open air. Device optimization is underway to introduce a more suitable hole-transport material and interfacial treatments to further improve the efficiencies, brightness and stability of our colloidal solution processed QD LEDs.

In summary, colloidal $CH_3NH_3PbBr_3$ perovskite QDs have been synthesized by addition of a demulsifier to $CH_3NH_3PbBr_3$ colloidal solutions to control the precipitation process in the emulsion. By controlling the emulsion and demulsion process, we obtained size-tunable QDs from 2 to 8 nm. The resulting QDs can be extracted from the reaction solution through a controllable precipitation. We further explored the use of these purified perovskite QDs as a light emitter in EL devices. The relatively simple structure of ITO/PEDOT/QDs/TPBi/CsF/Al led to QDs-LEDs with promising EL performance comparable with or even better the reported thin film-based devices with similar device structure (see Table S1). Although the colloidal solution-processed QDs LED has already exhibited an EL performance with high color-purity better than the well-developed CdSe-based QD-LEDs,[22−24] there is room to

DOI: 10.1021/acsami.5b10373
ACS Appl. Mater. Interfaces 2015, 7, 28128−28133

significantly improve the efficiency by introducing suitable electron transport layer and optimizing the quality of the QD layer. The improved QD LEDs may find wide applications for thin film displays, solid-state lighting, and other solution-processed optoelectronic devices. Moreover, the emulsion synthesis is versatile and can be extended for the fabrication of inorganic halide perovskite nanocrystals.

■ ASSOCIATED CONTENT

Supporting Information

The Supporting Information is available free of charge on the ACS Publications website at DOI: 10.1021/acsami.5b10373.

Chemicals and synthesis of CH_3NH_3Br, $CH_3NH_3PbBr_3$ QDs, and $CsPbBr_3$ QDs; details of plotting ternary phase (DMF/OA/*n*-hexane) diagram; device fabrication and material characterization; analysis of size distribution of resultant QDs; typical XRD patterns of $CH_3NH_3PbBr_3$ QDs; additional absorption and PL spectra of $CH_3NH_3PbBr_3$ QDs; the material characterizations and optical spectra of $CsPbBr_3$ QDs; the AFM and SEM measurements of a typical EL device; comparison of the device performance with reported thin film-based devices (PDF)

■ AUTHOR INFORMATION

Corresponding Authors

*E-mail: hzzhong@bit.edu.cn.
*E-mail: qpei@seas.ucla.edu.

Author Contributions

#H. H. and F. Z. contributed equally to this work.

Funding

This work was supported by the National Basic Research Program of China (2013CB328804), Natural Science Foundation of China (21573018), Beijing Nova program (xx2014B040).

Notes

The authors declare no competing financial interest.

■ REFERENCES

(1) Stranks, S. D.; Snaith, H. J. Metal-Halide Perovskites for Photovoltaic and Light-Emitting Devices. *Nat. Nanotechnol.* **2015**, *10*, 391−402.

(2) Tan, Z. K.; Moghaddam, R. S.; Lai, M. L.; Docampo, P.; Higler, R.; Deschler, F.; Price, M.; Sadhanala, A.; Pazos, L. M.; Credgington, D.; Hanusch, F.; Bein, T.; Snaith, H. J.; Friend, R. H. Bright Light-Emitting Diodes based on Organometal Halide Perovskite. *Nat. Nanotechnol.* **2014**, *9*, 687−692.

(3) Kim, Y. H.; Cho, H.; Heo, J. H.; Kim, T. S.; Myoung, N.; Lee, C. L.; Im, S. H.; Lee, T. W. Multicolored Organic/Inorganic Hybrid Perovskite Light-Emitting Diodes. *Adv. Mater.* **2015**, *27*, 1248−1254.

(4) Wang, J. P.; Wang, N. N.; Jin, Y. Z.; Si, J. J.; Tan, Z. K.; Du, H.; Cheng, L.; Dai, X. L.; Bai, S.; He, H. P.; Ye, Z. Z.; Lai, M. L.; Friend, R. H.; Huang, W. Interfacial Control toward Efficient and Low-Voltage Perovskite Light-Emitting Diodes. *Adv. Mater.* **2015**, *27*, 2311−2316.

(5) Qin, X.; Dong, H. L.; Hu, W. P. Green Light-Emitting Diode from Bromine based Organic-Inorganic Halide Perovskite. *Sci. China Mater.* **2015**, *58*, 186−191.

(6) Deschler, F.; Price, M.; Pathak, S.; Klintberg, L. E.; Jarausch, D. D.; Higler, R.; Hüttner, S.; Leijtens, T.; Stranks, S. D.; Snaith, H. J.; Atatüre, M.; Phillips, R. T.; Friend, R. H. High Photoluminescence Efficiency and Optically Pumped Lasing in Solution-Processed Mixed Halide Perovskite Semiconductors. *J. Phys. Chem. Lett.* **2014**, *5*, 1421−1426.

(7) Xing, G. C.; Mathews, N.; Lim, S. S.; Yantara, N.; Liu, X. F.; Sabba, D.; Grätzel, M.; Mhaisalkar, S.; Sum, T. C. Low-Temperature Solution-Processed Wavelength-Tunable Perovskites for Lasing. *Nat. Mater.* **2014**, *13*, 476−480.

(8) Zhu, H. M.; Fu, Y. P.; Meng, F.; Wu, X. X.; Gong, Z. Z.; Ding, Q.; Gustafsson, M. V.; Trinh, M. T.; Jin, S.; Zhu, X. Y. Lead Halide Perovskite Nanowire Lasers with Low Lasing Thresholds and High Quality Factors. *Nat. Mater.* **2015**, *14*, 636−642.

(9) Niu, Y. W.; Zhang, F.; Bai, Z. L.; Dong, Y. P.; Yang, J.; Liu, R. B.; Zou, B. S.; Li, J. B.; Zhong, H. Z. Aggregation-Induced Emission Features of Organometal Halide Perovskites and Their Fluorescence. *Adv. Opt. Mater.* **2015**, *3*, 112−119.

(10) González-Carrero, S.; Galian, R. E.; Pérez-Prieto, J. Organometal Halide Perovskites: Bulk Low-Dimension Materials and Nanoparticles. *Part. Part. Syst. Charact.* **2015**, *32*, 709−720.

(11) Tian, Y. X.; Merdasa, A.; Unger, E.; Abdellah, M.; Zheng, K. B.; McKibbin, S.; Pullerits, T.; Yartsev, A.; Sundstrom, V.; Scheblykin, I. G. Enhanced Organo-Metal Halide Perovskite Photoluminescence from Nanosized Defect-Free Crystallites and Emitting Sites. *J. Phys. Chem. Lett.* **2015**, *6*, 4171−4177.

(12) Cho, H.; Jeong, S. H.; Park, M. H.; Kim, Y. H.; Wolf, C.; Lee, C. L.; Heo, J. H.; Sadhanala, A.; Myoung, N.; Yoo, S.; Im, S. H.; Friend, R. H.; Lee, T. W. Overcoming the Electroluminescence Efficiency Limitations of Perovskite Light-Emitting Diodes. *Science* **2015**, *350*, 1222−1225.

(13) Li, G. R.; Tan, Z. K.; Di, D. W.; Lai, M. L.; Jiang, L.; Lim, J. H. W.; Friend, R. H.; Greenham, N. C. Efficient Light-Emitting Diodes based on Nanocrystalline Perovskite in a Dielectric Polymer Matrix. *Nano Lett.* **2015**, *15*, 2640−2644.

(14) Li, J. Q.; Bade, S. G. R.; Shan, X.; Yu, Z. B. Single-Layer Light-Emitting Diodes Using Organometal Halide Perovskite/Poly(ethylene oxide) Composite Thin Films. *Adv. Mater.* **2015**, *27*, 5196−5205.

(15) Wong, A. B.; Lai, M. L.; Eaton, S. W.; Yu, Y.; Lin, E.; Dou, L. T.; Fu, A.; Yang, P. D. Growth and Anion Exchange Conversion of $CH_3NH_3PbX_3$ Nanorod Arrays for Light-Emitting Diodes. *Nano Lett.* **2015**, *15*, 5519−5524.

(16) Schmidt, L. C.; Pertegás, A.; González-Carrero, S.; Malinkiewicz, O.; Agouram, S.; Mínguez Espallargas, G.; Bolink, H. J.; Galian, R. E.; Pérez-Prieto, J. Nontemplate Synthesis of $CH_3NH_3PbBr_3$ Perovskite Nanoparticles. *J. Am. Chem. Soc.* **2014**, *136*, 850−853.

(17) Hassan, Y.; Song, Y.; Pensack, R. D.; Abdelrahman, A. I.; Kobayashi, Y.; Winnik, M. A.; Scholes, G. D. Structure-Tuned Lead Halide Perovskite Nanocrystals. *Adv. Mater.* **2015**, 10.1002/adma.201503461.

(18) Zhang, F.; Zhong, H. Z.; Chen, C.; Wu, X. G.; Hu, X. M.; Huang, H. L.; Han, J. B.; Zou, B. S.; Dong, Y. P. Brightly Luminescent and Color-Tunable Colloidal $CH_3NH_3PbX_3$ (X = Br, I, Cl) Quantum Dots: Potential Alternatives for Display Technology. *ACS Nano* **2015**, *9*, 4533−4542.

(19) Gonzalez-Carrero, S.; Galian, R. E.; Pérez-Prieto, J. Maximizing the Emissive Properties of $CH_3NH_3PbBr_3$ Perovskite Nanoparticles. *J. Mater. Chem. A* **2015**, *3*, 9187−9193.

(20) Huang, H.; Susha, A. S.; Kershaw, S. V.; Hung, T. F.; Rogach, A. L. Control of Emission Color of High Quantum Yield $CH_3NH_3PbBr_3$ Perovskite Quantum Dots by Precipitation Temperature. *Adv. Sci.* **2015**, *2*, 10.1002/advs.201500194.

(21) Tyagi, P.; Arveson, S. M.; Tisdale, W. A. Colloidal Organohalide Perovskite Nanoplatelets Exhibiting Quantum Confinement. *J. Phys. Chem. Lett.* **2015**, *6*, 1911−1916.

(22) Sun, Q. J.; Wang, Y. A.; Li, L. S.; Wang, D. Y.; Zhu, T.; Xu, J.; Yang, C. H.; Li, Y. F. Bright, Multicoloured Light-emitting Diodes based on Quantum Dots. *Nat. Photonics* **2007**, *1*, 717−722.

(23) Shirasaki, Y.; Supran, G. J.; Bawendi, M. G.; Bulović, V. Emergence of Colloidal Quantum-Dot Light-Emitting Technologies. *Nat. Photonics* **2013**, *7*, 13−23.

(24) Dai, X. L.; Zhang, Z. X.; Jin, Y. Z.; Niu, Y.; Cao, H. J.; Liang, X. Y.; Chen, L. W.; Wang, J. P.; Peng, X. G. Solution-Processed, High-Performance Light-Emitting Diodes based on Quantum Dots. *Nature* **2014**, *515*, 96−99.

DOI: 10.1021/acsami.5b10373
ACS Appl. Mater. Interfaces 2015, 7, 28128−28133

(25) Malik, M. A.; Wani, M. Y.; Hashim, M. A. Microemulsion method: A Novel Route to Synthesize Organic and Inorganic Nanomaterials. *Arabian J. Chem.* **2012**, *5*, 397−417.
(26) Pileni, M. P. The Role of Soft Colloidal Templates in Controlling the Size and Shape of Inorganic Nanocrystals. *Nat. Mater.* **2003**, *2*, 145−150.
(27) Zheng, K. B.; Zhu, Q. S.; Abdellah, M.; Messing, M. E.; Zhang, W.; Generalov, A.; Niu, Y. R.; Ribaud, L.; Cnton, S. E.; Pullerits, T. Exciton Binding Energy and the Nature of Emissive States in Organometal Halide Perovskites. *J. Phys. Chem. Lett.* **2015**, *6*, 2969−2975.
(28) Sichert, J. A.; Tong, Y.; Mutz, N.; Vollmer, M.; Fischer, S.; Milowska, K. Z.; Cortadella, R. G.; Nickel, B.; Cardena-Daw, C.; Stolarczyk, J. K.; Urban, A. X.; Feldmann, J. Quantum Size Effect in Organometal Halide Perovskite Nanoplates. *Nano Lett.* **2015**, *15*, 6521−6527.

DOI: 10.1021/acsami.5b10373
ACS Appl. Mater. Interfaces 2015, 7, 28128−28133